Neurobiology of Stress 33 (2024) 100680

Contents lists available at ScienceDirect

Neurobiology of Stress

journal homepage: www.elsevier.com/locate/ynstr

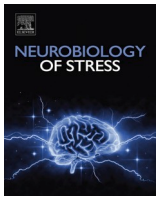

Cholecystokinin-expressing interneurons mediated inhibitory transmission and plasticity in basolateral amygdala modulate stress-induced anxiety-like behaviors in mice

Wei Fang [a,b], Xi Chen [a,b], Jufang He [a,b,c,*]

[a] Department of Neuroscience, City University of Hong Kong, Kowloon, Hong Kong
[b] Department of Biomedical Sciences, City University of Hong Kong, Kowloon, Hong Kong
[c] City University of Hong Kong Shenzhen Research Institute, Shenzhen, People's Republic of China

ARTICLE INFO

Handling Editor: Prof R Lawrence Reagan

Keywords:
Cholecystokinin interneurons
Anxiety
Acute stress
Inhibitory transmission
Inhibitory plasticity
Mice

ABSTRACT

The basolateral amygdala (BLA) hyperactivity has been implicated in the pathophysiology of anxiety disorders. We recently found that enhancing inhibitory transmission in BLA by chemo-genetic activation of local interneurons (INs) can reduce stress-induced anxiety-like behaviors in mice. Cholecystokinin interneurons (CCK-INs) are a major part of INs in BLA. It remains unknown whether CCK-INs modulated inhibition in BLA can mediate anxiety. In the present study, we found that BLA CCK-INs project extensively to most local excitatory neurons. Activating these CCK-INs using chemo-genetics and optogenetics can both effectively suppress electrical-induced neuronal activity within the BLA. Additionally, we observed that direct and sustained activation of CCK-INs within the BLA via chemo-genetics can mitigate stress-induced anxiety-like behaviors in mice and reduce stress-induced hyperactivity within the BLA itself. Furthermore, augmenting inhibitory plasticity within the BLA through a brief, 10-min high-frequency laser stimulation (HFLS) of CCK-INs also reduce stress-induced anxiety-like behaviors in mice. Collectively, these findings underscore the pivotal role of BLA CCK-IN-mediated inhibitory transmission and plasticity in modulating anxiety.

1. Introduction

Though low-to-moderate stress is beneficial to us in many aspects, including boosting our immune system and cognitive functions (Dooley et al., 2017; Oshri et al., 2022), intensive stress can elicit negative physical (e.g., sleep loss) and mental issues (e.g., anxiety) (Di et al., 2016; Wright et al., 2023). A previous epidemiological research revealed around 33.7% of people were diagnosed with anxiety disorders at least once during their lifetime (Bandelow and Michaelis, 2015), adversely affecting their life quality (Lochner et al., 2003).

The stress-induced hyperactivity in the basolateral amygdala (BLA) has been implicated in the pathophysiology of anxiety, which could result from the deficiency of local GABAergic control (Möhler, 2012; Prager et al., 2016; Zhang et al., 2023). Normalizing or enhancing the GABAergic inhibition may be regarded as a novel treatment strategy for anxiety. A recent study found enhancing GABAergic inhibition by chemo-genetics or optogenetics in BLA can alleviate anxiety-like behaviors in mice (Asim et al., 2023). It suggests a causal relationship between BLA hyperactivity and anxiety. GABAergic interneurons (INs) in BLA include three major and non-overlapped types of INs: parvalbumin (PV), somatostatin (SST), and cholecystokinin (CCK) INs (Kemppainen and Pitkänen, 2000; Vereczki et al., 2021). While CCK and PV INs mainly target on the perisomatic region of pyramidal neurons, SST INs innervate the distal dendrites (Muller et al., 2007; Rainnie et al., 2006). Previous research has found that chemo-genetic activation of PV-INs in BLA failed to affect anxiety-like behaviors in mice (Luo et al., 2020). Activation of SST-INs by intra-amygalar infusion of SST 14 and SST 28 can reduce anxiety-like behaviors in mice (Yeung et al., 2011). However, for CCK-INs, no study directly manipulates them in BLA to see whether it can regulate anxiety. Some have proposed the critical role of CCK-INs in regulating mood disorders (e.g., anxiety) (Babaev et al., 2018; Freund, 2003). Lesion of neurokinin1 expressing INs which highly co-express with CCK can cause anxiety-like behaviors in mice (Truitt et al., 2009). Thus, we hypothesize that activation of CCK-INs can produce anxiolytic effects.

In this study, we first revealed that CCK-INs send abundant

* Corresponding author. Department of Neuroscience, To Yuen Building, City University of Hong Kong, Tat Chee Avenue, Kowloon, Hong Kong.
E-mail address: jufanghe@cityu.edu.hk (J. He).

https://doi.org/10.1016/j.ynstr.2024.100680
Received 12 June 2024; Received in revised form 24 September 2024; Accepted 15 October 2024
Available online 16 October 2024

projections to most excitatory neurons in BLA. Both chemo-genetic and optogenetic activation of CCK-INs in BLA can suppress the electrical-induced neuronal activities in BLA. We further found direct and long-lasting activation of CCK-INs in BLA by chemo-genetics can alleviate stress-induced anxiety-like behaviors in mice as well as reduce stress-induced BLA hyperactivity. Moreover, we discovered inducing the inhibitory plasticity in BLA by 10-min HFLS of CCK-INs in BLA can also produce anxiolytic effects. Together, these findings indicate that CCK-INs-mediated inhibitory transmission and plasticity in BLA are critical in anxiety regulation.

2. Materials and methods

2.1. Animals

All experimental procedures were reviewed and approved by the Animal Subjects Ethics Sub-Committees of the City University of Hong Kong. Adult male CCK-ires-Cre (Ccktm1.1(Cre)Zjh/J, C57BL/6 background, for short CCK-Cre, Jackson Laboratory) were used for immunohistochemistry, in vitro electrophysiological recordings, and behavioral experiments. Adult male C57BL/6 mice were used for immunohistochemistry. Mice for behavioral tests were housed in 12 h light/12 h dark cycles (dark from 8:00 to 20:00) and given food and water ad libitum. All behavioral tests were carried out during the period of darkness.

2.2. Viral vectors

The following adeno-associated virus (AAV) vectors were used in my current study: rAAV-mDlx-DIO-ChrimsonR-BFP-WPRE-hGHPA, rAAV-mDlx-DIO-mCherry, and rAAV-mDlx-DIO-hM3D(Gq)-mCherry-WPRE-hGH-pA, which were purchased from BrainVTA. They were diluted to the appropriate titer (approximately 5×10^{12} vg/ml) with artificial cerebrospinal fluid before injection.

2.3. Drugs

The following drugs were used in our current study: sulfated cholecystokinin-8 (CCK8s, Go Top Peptide Biotech), clozapine N-oxide (CNO, ApexBio), and devazepide (MedChemExpress).

2.4. Stereotaxic viral injection, optical fiber, and drug cannula implantation

Mice were anesthetized by pentobarbital sodium (50 mg/kg, intraperitoneal injection) for stereotaxic viral injection into bilateral BLA (AP: 1.60 mm from the bregma; ML: ±3.40 mm from the bregma; DV = −4.00 mm from the dura matter). After performing craniotomy on a stereotaxic device, 300 nl of the virus was injected through a glass needle connected with the Nanoliter2000 system (World Precision Instruments) at a rate of 50 nl/min. After injection, the glass needle was left in the injection site for 10 min before gradually withdrawing. Then, the scalp was sutured, and erythromycin ointment was applied to the m. The animal was returned to its home cage after awakening on a 37°C-heat pad.

To implant fiber-optic cannulas (200 μm, 0.37 NA, Inper) or drug cannulas (OD = 0.41 mm, RWD Life Science), each piece was slowly inserted into the bilateral BLA after the virus injection and gently fixed by applying adhesive cement (C&B Metabond) and dental cement (mega PRESS NV + JET X) afterward. The coordinates were the same as the virus injection except that the DV changed to −3.85 mm. For drug cannula implantation, a dummy cannula was inserted into the guide cannula to provide protection. After waking on the heat pad, mice were returned to their home cages.

2.5. Drug infusion and HFLS in the behavioral tests

To infuse the drug, two 10 μL syringes (Hamilton) were connected with the injection cannula (RWD Life Science) through two soft PE tubes (RWD Life Science), respectively. The drug infusion was controlled by a dual syringe pump (Hamilton) at a speed of 250 nl/min. The volume for each side of BLA is 500 nl. Mice were allowed to move freely during the drug infusion.

Before performing HFLS (20 Hz, 2 ms in duration, 600 pulses) to stimulate CCK-INs in bilateral BLA, we used an optical fiber (200 μm, 0.37 NA, Inper) to connect the fiber-optic cannulas and the 635 nm laser machine (Inper). Mice were allowed to move freely during the stimulation.

2.6. In vitro electrophysiology

For brain slices preparation, animals were deeply anesthetized with isoflurane and coronal sections (300 μm thick) across BLA were cut using a vibratome in well-oxygenated (95% O2/5% CO2, v/v) ice-cold artificial cerebrospinal fluid (ACSF: 124 mM NaCl, 2.5 mM KCl, 1 mM NaH2PO4, 10 mM D-glucose, 25 mM NaHCO3, 2 mM CaCl2, and 1 mM MgCl2, at pH 7.35–7.45). The brain slices recovered for 1.5h at 30 ± 1 °C in oxygenated ACSF. After recovery, one slice was put on the probe (MED-PG515A, Alpha MED Scientific Inc.) to make sure the area of BLA was attached to the 16-channel array by using a light microscope. Once the slice was fixed, a fine mesh and slice anchor (Warner Instruments) were carefully and sequentially placed on top of the slice to ensure slice stabilization during the recording. At the same time, the slice was constantly perfused with oxygenated 30 ± 1°CACSF through a peristaltic pump. To select the best stimulation electrode for electrical stimulation (ES), monopolar and biphasic constant-current pulses (0.2 ms in duration) were given by the data acquisition software Mobius (Alpha MED Scientific Inc.) with a 3s interval. The field excitatory postsynaptic potentials (fEPSPs) were recorded at the remaining electrodes and then amplified and shown on the monitor screen.

In the optogenetics-involved experiments, a 635 nm laser (3–5 mW, 2 ms in duration) was given by an optogenetic equipment (Inper) through an optic fiber (200 μm, 0.37 NA, Inper) whose tip was immersed into ACSF containing probe with around 300 mm away from the slice. After recording the stable ES evoked fEPSPs for at least 15 min as a baseline (e.g., the deviation did not exceed 10% of the average amplitude), the laser was given 20 ms before the ES. This paired stimulation lasted for at least 15 min until another stable ES-evoked fEPSPs was achieved. Next, vehicle or drug (CCK8s/devazepide) diluted in ACSF was perfused for 10 min before high-frequency laser stimulation (HFLS, 10 pulses at 20 Hz, repeated for 10 trials at 0.1 Hz) or low-frequency laser stimulation (LFLS, 100 pulses at 1 Hz) was introduced. At last, the pair of stimulations was presented again and the ES-evoked fEPSP responses were recorded for at least 60 min. We normalized the fEPSP amplitudes as a percentage change from the baseline. We compared the average normalized amplitudes during the last 10 min before HFLS/LFLS with those recorded in the last 10 min after HFLS/LFLS to assess whether the laser-induced inhibition was potentiated. We also compare the group differences in normalized amplitudes before HFLS/LFLS to confirm the magnitudes of optogenetic inhibition in different groups are similar.

Adapted from Su et al., (2023), in the chemo-genetics involved experiment, 50 μM CNO diluted in ACSF was perfused for 20 min after the ES-evoked fEPSPs were stable for at least 15 min (baseline). Then, CNO was washed out and we recorded ES evoked fEPSPs for at least 60 min. We also normalized the fEPSPs amplitudes as a percentage change from the baseline. We compared the normalized amplitudes of fEPSPs every 15 min after the CNO perfusion with the baseline.

2.7. Anatomy and immunohistochemistry

After the in-vitro electrophysiological recordings, we removed the slice from the recording probe and mount it on a slide. The viral expression of the slice was then checked through a Ni-E upright fluorescence microscope (Nikon).

To observe cannula positions and perform immunohistochemistry, mice were first deeply anesthetized with over-dose pentobarbital (100 mg/kg, intraperitoneal injection) and then perfused transcardially with 30 ml ice-cold phosphate-buffered saline (PBS) and fixed with 20 ml 4% paraformaldehyde (PFA) in PBS. The whole brain was taken out and put into 15 ml 4% PFA in PBS at 4 °C overnight and then transferred to 30% sucrose solution until the brain sank to the bottom. Coronal sections (30 μ m) were cut and stored in PBS by using a cryostat (Epredia™ HM525 NX Cryostat). To perform the immunohistochemistry, slices were washed 3 times in PBS for 7 min at a time and blocked by a blocking buffer containing 5% normal goat serum in 0.3% Triton X-100/PBS (PBST) for 1.5hr at room temperature. After blocking, slices were incubated with primary antibodies in blocking buffer overnight at 4 °C. Then, slices were washed with PBS for another 3 times of 7 min. Next, slices were stained with a secondary antibody at room temperature for 3 h. Afterward, the slices were washed with PBS for 3 × 7 min. At last, slices were mounted onto the slides.

To observe synaptic connections between pyramidal neurons and CCK-GABAergic neurons in BLA, we adopted Leica STELLARIS 8 lightning to obtain images with better resolution and clarity (Nonaka et al., 2024). We defined synapses if presynaptic terminals from CCK-INs colocalized with postsynaptic markers "Gephyrin" (Babij et al., 2023). If we observe functional synapses around local CaMKIIα labeled pyramidal neurons, these pyramidal neurons are regarded to receive local CCK-GABAergic projections. All the other microscope images were captured by Nikon AXR confocal microscope and analyzed by ImageJ.

The primary antibodies targeting GPR173 (1:1000, Invitrogen, PA5-50976), GAD67 (1:500, Sigma-Aldrich, MAB5406), CaMKIIα (1:500, Invitrogen, MA1048; 1:100, Abcam, ab131468), Gephyrin (1:200, Synaptic systems 147 318), c-Fos (1:1000, Abcam, ab190289), CCK (1:500, Abcam, ab37274) and the secondary antibodies including Alexa Fluor 488 (1:200, Jackson Immunoresearch, 111-545-003; 1:200, Abcam, ab150185), Alexa Fluor 647 (1:200, Abcam, ab150187; 1:200, Jackson Immunoresearch, 711-605-152), and Atto 647N (1:200, Sigma Aldrich, 40839) were used in this study.

We calculated the percentage of excitatory neurons receiving local CCK-GABAergic projections in BLA. We also analyzed the percentage of colocalization between excitatory neurons (marker: CaMKIIα) and GPR173 neurons, and colocalization between inhibitory neurons (marker: GAD67) and GPR173 neurons in BLA. To assess c-Fos expression, we calculated the number of c-Fos cells per millimeter square. The n in the figures indicates the number of representative biological replicates, and N indicates the number of independent animals.

2.8. Acute restraint stress (ARS)

We randomly selected two or three mice from a vivarium as stressed mice, and the rest of mice in the cage were defined as non-stressed mice. Prior to the restraint, we put the cages in the experimental room with dim light for 30 min as habituation. Stressed mice were individually subjected to a restraint device that could tightly restrain their body for 2 h (Liu et al., 2023; Novaes et al., 2018). After the restraint, mice were returned to their home cages until behavioral tests. The unstressed counterparts were subjected to the same handling and habituation procedures and remained undisturbed in their home cages until the behavioral tests (Mustafa et al., 2015; Lee et al., 2021).

2.9. Open field test (OFT)

Mice were placed in the center of an open field (50 cm length, 50 cm width, 40 cm height) with dim light and allowed to freely move for 10 min (Seibenhener and Wooten, 2015). Their moving paths were recorded by a video camera and analyzed with Smart 3.0 software. Locomotor activity was evaluated as the total distance it travelled; anxiety level was assessed by accumulating the time it spent in the central zone (30 × 30 cm).

2.10. Elevated plus maze (EPM)

The equipment was custom-made using dark black plastic boards with two open arms (25 × 5 × 0.5 cm) and two closed arm (25 × 5 × 16 cm). They were perpendicular to each other with a center platform (5 × 5 × 0.5 cm). The maze is elevated 50 cm from the ground. Mice were placed at the center gently, with their heads pointing to the open arm and opposite the experimenter. Mice were allowed to explore for 5 min. The anxiety level was assessed by calculating the number of entries into closed-arms, and the total time spent in closed-arms (Walf and Frye, 2007).

2.11. Statistical analyses

Data are shown as means ± SEM. Data were analyzed by GraphPad Prism 8.0.1. To compare group differences between two independent groups, an unpaired *t*-test was employed. One-way ANOVA and repeated measures (RM) ANOVA were performed to compare multiple group differences. Bonferroni correction was adopted for multiple comparison tests.

3. Results

3.1. Most excitatory neurons in BLA receive projections from local CCK-INs

In BLA, the activities of excitatory neurons are mediated by local GABAergic circuits (Spampanato et al., 2011). To further characterize the synaptic connections between excitatory neurons and CCK-INs in BLA, we adopted viral injection to label CCK-INs in BLA by injecting "rAAV-mDlx-DIO-mCherry-pA" into BLA of CCK-Cre mice (Fig. 1A). After four-week expression, we performed immunohistochemistry to visualize the excitatory neurons (marker: CaMKIIα) and their synaptic connections (marker: gephyrin) (Fig. 1B) in BLA. We first observed lots of CCK-GABAergic terminals around CaMKIIα positive neurons in BLA and then we randomly selected 15–17 neurons to check whether gephyrin puncta was colocalized with CCK-GABAergic terminals (Ippolito and Eroglu, 2010). We found that around 73.33% ± 2.99% of excitatory neurons in BLA received local CCK-GABAergic projection (Fig. 1C), which is consistent with previous research (Vereczki et al., 2016). Moreover, we found the virus can efficiently label CCK-INs in BLA because we stained the virus-infected BLA slices with CCK antibody and found 81.78% ± 2.04% of CCK-INs co-expressed CCK (Fig. 1D & E).

3.2. Chemo-genetic activation of CCK-INs can suppress the local neural activities induced by electrical stimulation

Considering the abundant synaptic projections from CCK-INs to excitatory neurons in BLA, we next investigated whether chemo-genetic activation of CCK-INs in BLA can inhibit local neural activities induced by electrical stimulation.

We selectively expressed hM3D(Gq), an engineered excitatory G protein-coupled receptor that can excite neuronal activities in the presence of CNO, in BLA CCK-INs by injecting rAAV-mDlx-DIO-hM3D (Gq)-mCherry into the BLA of adult CCK-Cre mice (Fig. 2A and B). As a control, we also injected its control virus rAAV-mDlx-DIO-mCherry into the BLA of their littermates (Fig. 2A and B). After at least three weeks of expression, in vitro multielectrode array recordings were employed (Fig. 2C).

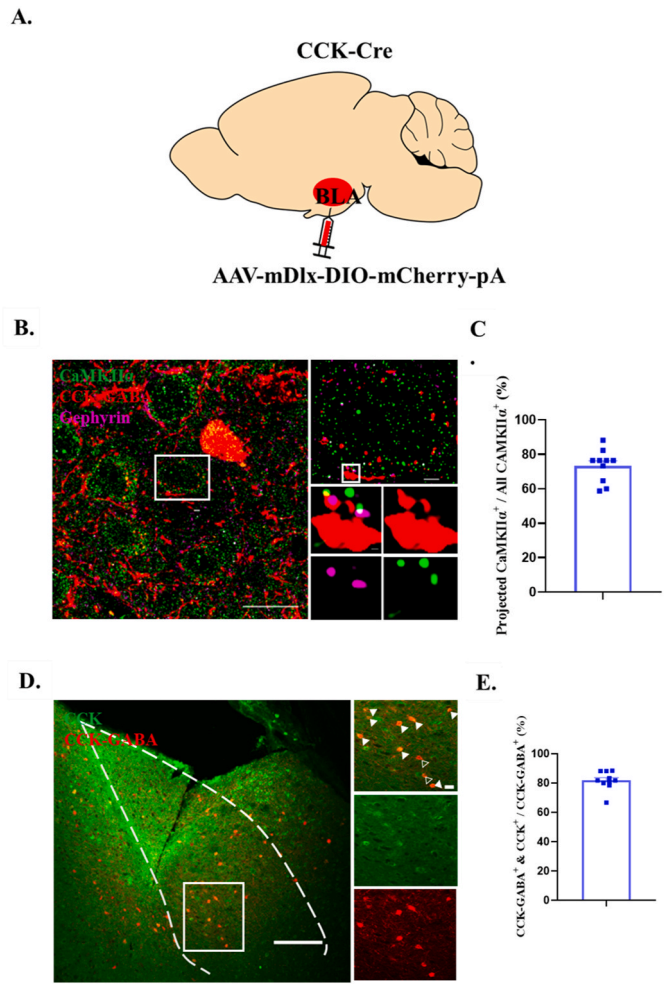

Fig. 1. Most excitatory neurons receive projections from local CCK-INs. **A,** Injection of AAV-mDlx-DIO-mCherry-pA into BLA of CCK-Cre mice. **B,** Representative images acquired with a 100 × objective and Leica lightning deconvolution show virus-infected CCK-GABAergic neurons and their terminals (red), glutamatergic neurons (CaMKIIα, green), and inhibitory postsynaptic marker (gephyrin, magenta). **C,** The bar chart shows the percentage (73.33% ± 2.99%) of excitatory neurons receiving projections from local CCK-INs. N = 3 mice, n = 10 slices (15–17 neurons for each slice). **D,** Representative images acquired with a 20 × objective show the overlay between virus-infected CCK-GABA neurons and CCK positive neurons. **E,** The bar chart shows the percentage (81.78% ± 2.04%) of overlay neurons positive for CCK-GABA and CCK in CCK-Cre mice. N = 3 mice, n = 10 slices. Scale bars: 20 μm, 2 μm and 0.2 μm for panel B; 200 μm and 20 μm for panel D. Data are shown as Mean ± SEM.

We found a significant main effect of time, F (2.07, 16.58) = 11.06, p = 0.0008. Overall, ES-induced neuronal activities in BLA were suppressed by chemo-genetic activation of local CCK-INs and the suppression effect lasted for at least 45 min during the wash-out period and disappeared later (Fig. 2D). Bonferroni's post hoc analyses revealed that in the hM3D(Gq) group, during the CNO perfusion, the local neural activities aroused by ES were significantly suppressed as the normalized amplitudes of fEPSP were reduced compared to the baseline (baseline vs. CNO: 100% vs. 90.3 ± 2.63%, p = 0.0309. See Fig. 2D–F). Then, CNO was washed out, but the suppression effect lasted for the next 45 min (baseline vs. 1–15 min post-CNO: 100% vs. 87.06% ± 2.12%, p = 0.0015; baseline vs. 16–30 min post-CNO: 100% vs. 91.6% ± 2.11%, p = 0.0202; baseline vs. 31–45 min post-CNO: 100% vs. 95.69% ± 1.14%, p = 0.0268. See Fig. 2D–F). Later, the ES-induced neural activities returned to the baseline level (baseline vs. 46–60 min post-CNO: 100% vs. 96.11% ± 1.72, p = 0.2674. See Fig. 2D–F). In the control group, CNO perfusion did not affect the ES induced neural activities in any phase (insignificant main effect of time windows: F (1.78, 12.49) = 2.72, p = 0.1087. Baseline vs. CNO vs. 1–15 min vs. 16–30 min vs. 31–45 min vs. 46–60 min: 100% vs. 100.1 ± 1.06% vs. 100% ± 1.73% vs. 102.2% ± 1.66% vs. 103.9% ± 1.71% vs. 103% ± 2.18, ps > 0.05. See Fig. 2D and E). These results suggest that chemo-genetic activation of CCK-INs in BLA can increase the local inhibitory transmission.

3.3. Enhancing inhibitory transmission in BLA by chemo-genetic activation of local CCK-INs can reduce stress-induced anxiety-like behaviors in mice

Through in-vitro electrophysiology, we confirmed the local inhibitory effect induced by chemo-genetic activation of CCK-INs in BLA, which was consistent with previous studies (Ballaz and Bourin, 2021). However, it remains unknown whether chemo-genetic activation of CCK-INs in BLA can produce an anxiolytic effect.

We first adopted an acute restraint stress (ARS) model to induce anxiety-like behaviors in mice and found stressed mice had more anxiety-like behaviors than the non-stressed mice (Fig. A1A), indicated by less center time in the open field test (OFT) (Fig. A1G, I; Stressed vs. Non-stressed: 104.3 ± 16.34 vs. 208.6 ± 40.63, t (14) = 2.38, p = 0.032), and less travelled time (Fig. A1B, F; Stressed vs. Nonstressed: 30.95 ± 10.29 vs. 95.32 ± 24.11, t (14) = 2.46, p = 0.0277) and entries in open arms in the elevated plus maze test (EPM) (Fig. A1C; Stressed vs. Nonstressed: 3.5 ± 0.63 vs. 7.75 ± 0.82, t (14) = 4.12, p = 0.001). They displayed no differences in travelled distance in both OFT (Fig. A1H; Stressed vs. Nonstressed: 28.54 ± 2.39 vs. 30.04 ± 2.1, t (14) = 0.47, p = 0.6434) and EPM (Fig. A1E; Stressed vs. Nonstressed: 9.33 ± 0.95 vs. 9.36 ± 0.76, t (14) = 0.03, p = 0.9792). They also showed no difference in the total number of entries in both arms (Fig. A1D; Stressed vs. Nonstressed: 15.63 ± 2.13 vs. 16.38 ± 1.43, t (14) = 0.29, p = 0.7741). Stressed mice had more active BLA than non-stressed mice, as indicated by more intense c-Fos signals in BLA (Stressed vs. Non-stressed: 371.5 ± 52.57 vs. 237.3 ± 22.54, t (17) = 2.26, p = 0.0376; Fig. A1J, K). These results indicate that the ARS we adopted in our study can induce anxiety-like behaviors in mice and cause BLA hyperactivity.

We injected the viruses "rAAV-mDlx-DIO-hM3D(Gq)-mCherry" or "rAAV-mDlx-DIO-mCherry" into both sides of BLA of CCK-Cre mice respectively (Fig. 3A and B). After 3-week virus expression, we started to test the anxiolytic effects of chemo-genetic activation of CCK-INs in BLA. Mice first received 2-hr ARS and returned to their home cages to rest for 30 min until 500 nl CNO (3 μmol) were infused into both sides of BLA (Fig. 3A). After the CNO infusion, mice were put back in their home cages for another 30 min before the behavioral tests. Once the behavioral tests were finished, we performed the trans-cardiac perfusion for the mice brains. Afterward, we prepared the brain slices and performed the c-Fos staining of BLA slices.

After ARS, mice receiving chemo-genetic activation of CCK-INs in BLA had more travel time (Fig. 3C–G; mCherry vs. hM3D(Gq): 38.46 ± 5.83 vs. 75.7 ± 10.03, t (15) = 3.11, p = 0.0072) and entries in open arms (Fig. 3D; mCherry vs. hM3D(Gq): 4.88 ± 0.55 vs. 7.78 ± 1.13, t (15) = 2.22, p = 0.0421) than the mCherry mice in the elevated plus maze test. But in general, their total entries in both open and closed arms were similar (Fig. 3E; mCherry vs. hM3D(Gq): 15.38 ± 1.15 vs. 18.67 ± 2.76, t (15) = 1.05, p = 0.3102). Moreover, their travelled distance was also similar (Fig. 3F; mCherry vs. hM3D(Gq): 9.27 ± 0.49 vs. 11.51 ± 1.74, t (15) = 1.17, p = 0.2591). In the open field test, they displayed more travel time in the center (Fig. 3H–J; mCherry vs. hM3D(Gq): 57.53 ± 12.29 vs. 142.4 ± 31.05, t (15) = 2.42, p = 0.0284) but had similar locomotion than the controls (Fig. 3I; mCherry vs. hM3D(Gq): 26.34 ± 2.45 vs. 27.66 ± 1.15, t (15) = 0.51, p = 0.6198). We also found weaker c-Fos signals in hM3D(Gq) mice than mCherry mice (Fig. 3K and L; mCherry vs. hM3D(Gq): 597.5 ± 42.6 vs. 337 ± 35.14, t (22) = 4.78, p < 0.0001), indicating chemo-genetic activation of CCK-INs in BLA can significantly reduce stress-induced BLA hyperactivity. However, chemo-genetic activation of CCK-INs in BLA failed to significantly affect the

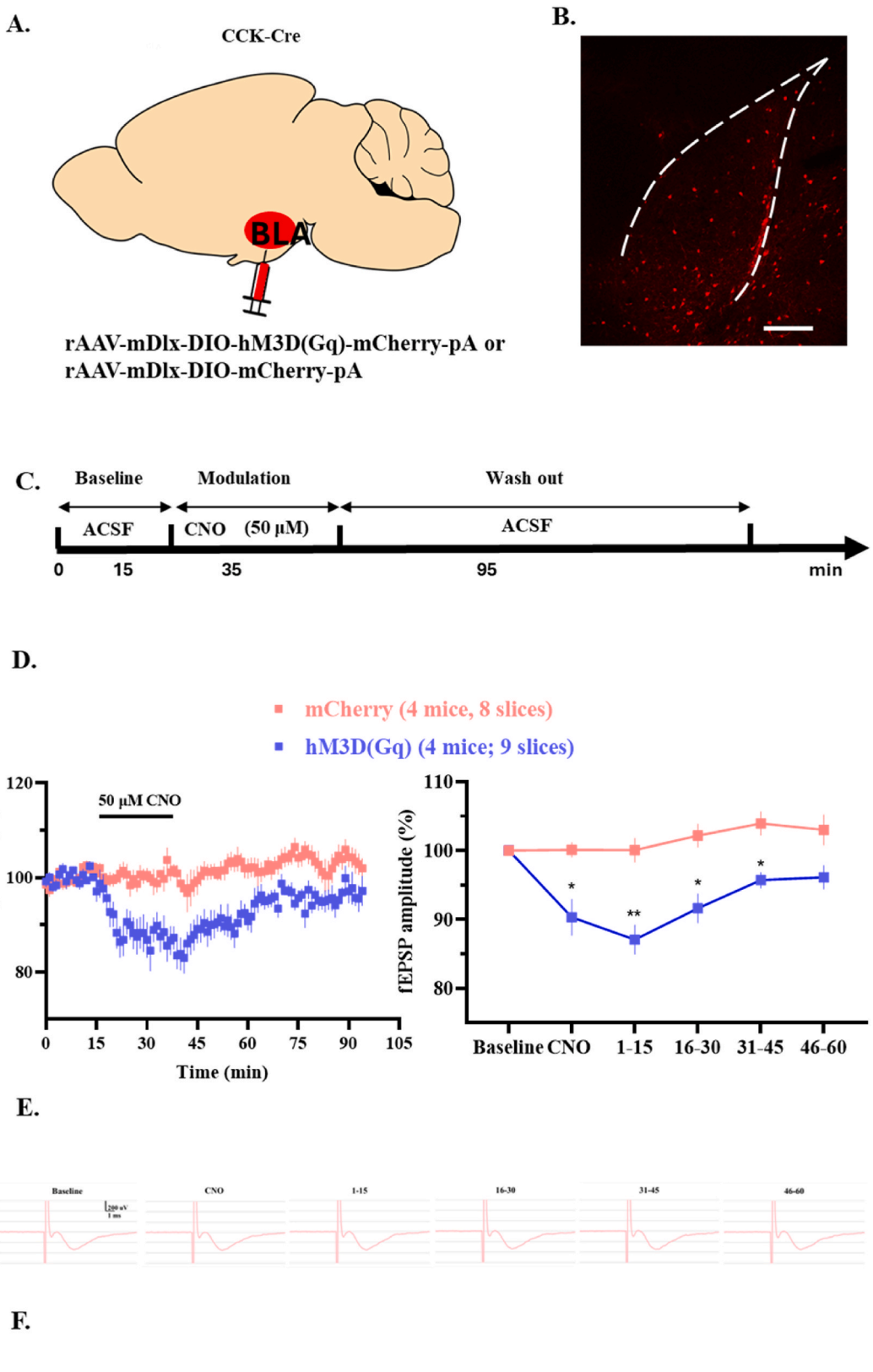

(caption on next page)

Fig. 2. Chemo-genetic activation of CCK-INs can suppress the local neural activities induced by electrical stimulation.
A, A schematic diagram shows the injection of "rAAV-mDlx-DIO-hM3D(Gq)-mCherry-pA" or its control virus "rAAV-mDlx-DIO-mCherry-pA" into the BLA of CCK-Cre mice. **B,** A representative image shows the virus expression. **C,** A flow chart shows the protocol we adopted for this experiment. **D,** Left panel: the line chart shows the time course of average normalized amplitudes of fEPSP in the hM3D(Gq) (blue) and mCherry (pink) groups respectively. Right panel: the bar chart shows the average normalized amplitudes of fEPSP in different time windows. In the hM3D(Gq) group, there was a significant main effect of time windows, $F(2.07, 16.58) = 11.06$, $p = 0.0008$; Bonferroni's post hoc analyses revealed that compared with the baseline, ES-induced neural activities were significantly suppressed by chemo-genetic activation of CCK-INs in BLA ($p < 0.05$) and the suppression effect lasted 45 min after CNO perfusion (ps < 0.05). Then, fEPSP amplitudes returned to the baseline level ($p > 0.05$). In the mCherry group, there was no significant main effect of time windows, $F(1.78, 12.49) = 2.72$, $p = 0.1087$. Compared with the baseline, the average amplitudes in all the other time windows showed no differences (ps > 0.05). **E & F,** The representative fEPSP traces in different time windows in mCherry (Pink) and hM3D(Gq) (Blue) groups. mCherry & hM3D(Gq): N = 4 mice, n = 8 or 9 slices. $^{**}p < 0.01$; $^{***}p < 0.001$; ns: no significance. Scale bar: 200 μm. Data are shown as Mean ± SEM.

basal anxiety levels in mice (Fig. A5). Specifically, we found there was no significant difference between the time they spent in the open arms (Fig. A5B & F; mCherry vs. hM3D(Gq): 50.9 ± 8.64 vs. 87.18 ± 21.7, $t(12) = 1.55$, $p = 0.1462$) and open field areas (Fig. A5G & I; mCherry vs. hM3D(Gq): 112 ± 17.2 vs. 171 ± 39.56, $t(12) = 1.37$, $p = 0.1966$). There was also no difference between their entries in the open arms (Fig. A5C; mCherry vs. hM3D(Gq): 6.86 ± 1.1 vs. 8.86 ± 1.49, $t(12) = 1.08$, $p = 0.3009$) and both arms (Fig. A5D; mCherry vs. hM3D(Gq): 16.14 ± 1.93 vs. 18.43 ± 4.04, $t(12) = 0.51$, $p = 0.6191$). Their locomotion was also not affected by the manipulation in both tests (Fig. A5E, EPM: mCherry vs. hM3D(Gq): 9.57 ± 0.81 vs. 9.03 ± 1.56, $t(12) = 0.31$, $p = 0.762$; Fig. A5H, OFT: mCherry vs. hM3D(Gq): 28.52 ± 2.64 vs. 26.05 ± 2.3, $t(12) = 0.71$, $p = 0.4937$). There was no difference in the c-Fos expression in BLA (Fig. A5J & K; mCherry vs. hM3D(Gq): 377.1 ± 36.89 vs. 308.1 ± 32.53, $t(18) = 1.4$, $p = 0.1772$). In general, we could see a trend that hM3D(Gq) mice had lower anxiety-level than mCherry mice. Moreover, we also compared the anxiety-related behavioral outcomes between mCherry non-stressed mice and mCherry stressed mice. We found that mCherry non-stressed mice had more center time in OFT (mCherry non-stressed vs. mCherry stressed: 112 ± 17.2 vs. 57.53 ± 12.29, $t(13) = 2.63$, $p = 0.021$) and less c-Fos expression in BLA (mCherry non-stressed vs. mCherry stressed: 377.1 ± 36.89 vs. 597.5 ± 42.6, $t(20) = 3.83$, $p = 0.0011$) than mCherry stressed mice, suggesting ARS can also induce anxiety-like phenotypes and BLA hyperactivity in the chemo-genetic experiment. We did not find significant difference in other indices (e.g., entries in open arms, time spent in open arms etc., ps > 0.05). These results suggest that enhancing local inhibitory transmission by chemo-genetic activation of CCK-INs in BLA can alleviate stress-induced anxiety-like behaviors in mice as well as suppress BLA neuronal activities, without affecting their locomotion and basal anxiety levels.

3.4. HFLS but not LFLS of CCK-INs can induce iLTP in BLA

In the experiments above, we showed that direct and long-lasting activation of CCK-INs by chemo-genetics can produce anxiolytic effects by directly suppressing stress-induced neuronal hyperexcitation. The balance between excitation and inhibition can also be modulated by inhibitory plasticity (Vogels et al., 2011; Wu et al., 2022). The potentiation of inhibitory synapses contributes to the decrease in network firing rates (Miska et al., 2018; Nahmani and Turrigiano, 2014). So, it is likely that inducing long-term potentiation of inhibitory synapses (i.e., iLTP) in BLA can also cause anxiolytic effects. Previous research unveiled the induction of iLTP in the neocortex relies on the binding between CCK and its receptor GPR173, which can be triggered by high-frequency laser stimulation (HFLS) of CCK-INs (He et al., 2023). Here, we found the abundance of GPR173 in BLA (Fig. A2A), which mainly localized at glutamatergic neurons rather than GABAergic neurons (Fig. A2B, C, D). However, it remains unknown whether HFLS of CCK-INs in BLA can also induce iLTP. High-frequency stimulation is a typical protocol that induces long-term potentiation at inhibitory synapses (Creed et al., 2015; He et al., 2023), whereas only low-frequency stimulation rarely induces iLTP (Hawken et al., 2019). Here, we investigated whether HFLS of CCK-INs in BLA could induce iLTP. We adopted the low-frequency laser stimulation (LFLS) protocol as a control.

We injected rAAV-mDlx-DIO-ChrimsonR-BFP into the BLA of adult CCK-Cre mice (Fig. 4A and B). After at least three weeks of expression, in vitro multielectrode array recordings were employed (Fig. 4C). We calculated the change of the amplitudes of electrical stimulation (ES) induced fEPSPs to reflect the magnitude of inhibition caused by laser stimulation (LS) of CCK-INs. We expected that HFLS of CCK-INs could potentiate the inhibition caused by a single-pulse LS of CCK-INs for a long term, whereas LFLS of CCK-INs failed to trigger the iLTP.

We found optogenetic activation of CCK-INs can significantly inhibit the neural activities induced by ES in both conditions (Fig. 4D and E; in the HFLS condition, without LS vs. with LS: 100% ± 0.47% vs. 84.5% ± 3.17%, $p < 0.0001$; in the LFLS condition, without LS vs. with LS: 100.5% ± 0.26% vs. 85.51% ± 1.38%, $p < 0.0001$). Before applying HFLS or LFLS, the degree of inhibition did not show significant difference in these two conditions (Fig. 4D and E; HFLS vs. LFLS: 84.5% ± 3.17% vs. 85.51% ± 1.38%, $t(14) = 0.29$, $p = 0.7744$). After HFLS, BLA slices showed iLTP with the same LS (Fig. 4D and E; before HFLS vs. after HFLS: 84.5% ± 3.17% vs. 55.97% ± 3.38%, $p < 0.0001$). We also found that HFLS-induced iLTP can be blocked by GPR173 antagonists (Devazepide, 100 nM) in BLA (Fig. A3D, E; before HFLS vs. after HFLS: 82.46% ± 2.93% vs. 80.99% ± 4.91%, $p = 0.6762$). It suggests the induction of iLTP in BLA is GPR173 dependent. As expected, LFLS failed to trigger iLTP (Fig. 4D and E; before LFLS vs. after LFLS: 85.51% ± 1.38% vs. 85.71% ± 2.75%, $p = 0.9565$). However, we additionally added CCK8s (200 nM) before LFLS and found it can rescue the iLTP (Fig. A4D, E; before LFLS vs. after LFLS: 85.08% ± 2.39% vs. 62.17% ± 3.02%, $p = 0.0002$), which means the iLTP in BLA is also CCK dependent. In conclusion, these results indicate that HFLS of CCK-INs in BLA may induce CCK release, which would bind to GPR173 at glutamatergic neurons, triggering the induction of iLTP in BLA.

3.5. Inducing inhibitory plasticity by HFLS of CCK-INs in BLA can reduce stress-induced anxiety-like behaviors in mice

As HFLS of CCK-INs in BLA can induce iLTP, the next question is whether HFLS-induced iLTP in BLA can produce anxiolytic effects.

We injected rAAV-mDLX-DIO-ChrimsonR-BFP or its control virus rAAV-mDLX-DIO-mCherry into BLA of male CCK-Cre mice (Fig. 5A and B). Similarly, after three weeks of expression, mice would first receive 2-hr restraint stress and then we gave 10-min HFLS to their bilateral BLA CCK-INs (Fig. 5A). Mice were immediately returned to their home cages to rest for 50 min. Next, mice were tested for their anxiety levels. After the behavioral tests, we perfused the mice and performed the c-Fos staining of BLA slices.

Overall, we found inducing the inhibitory plasticity in BLA by HFLS of local CCK-INs can effectively reduce stress-induced anxiety-like behaviors in mice. Specifically, in the elevated plus maze test, ChrimsonR mice spent more time (Fig. 5C–G; mCherry vs. ChrimsonR: 15.03 ± 5.45 vs. 38.28 ± 6.84, $t(15) = 2.61$, $p = 0.0196$) and entered more often in open arms (Fig. 5D; mCherry vs. ChrimsonR: 3.5 ± 0.57 vs. 6 ± 0.44, $t(15) = 3.52$, $p = 0.0031$) than their control littermates, even though the numbers of their entries in both arms were similar (Fig. 5E; mCherry vs. ChrimsonR: 15.38 ± 2.58 vs. 19 ± 1.35, $t(15) = 1.29$, $p = 0.2175$) and

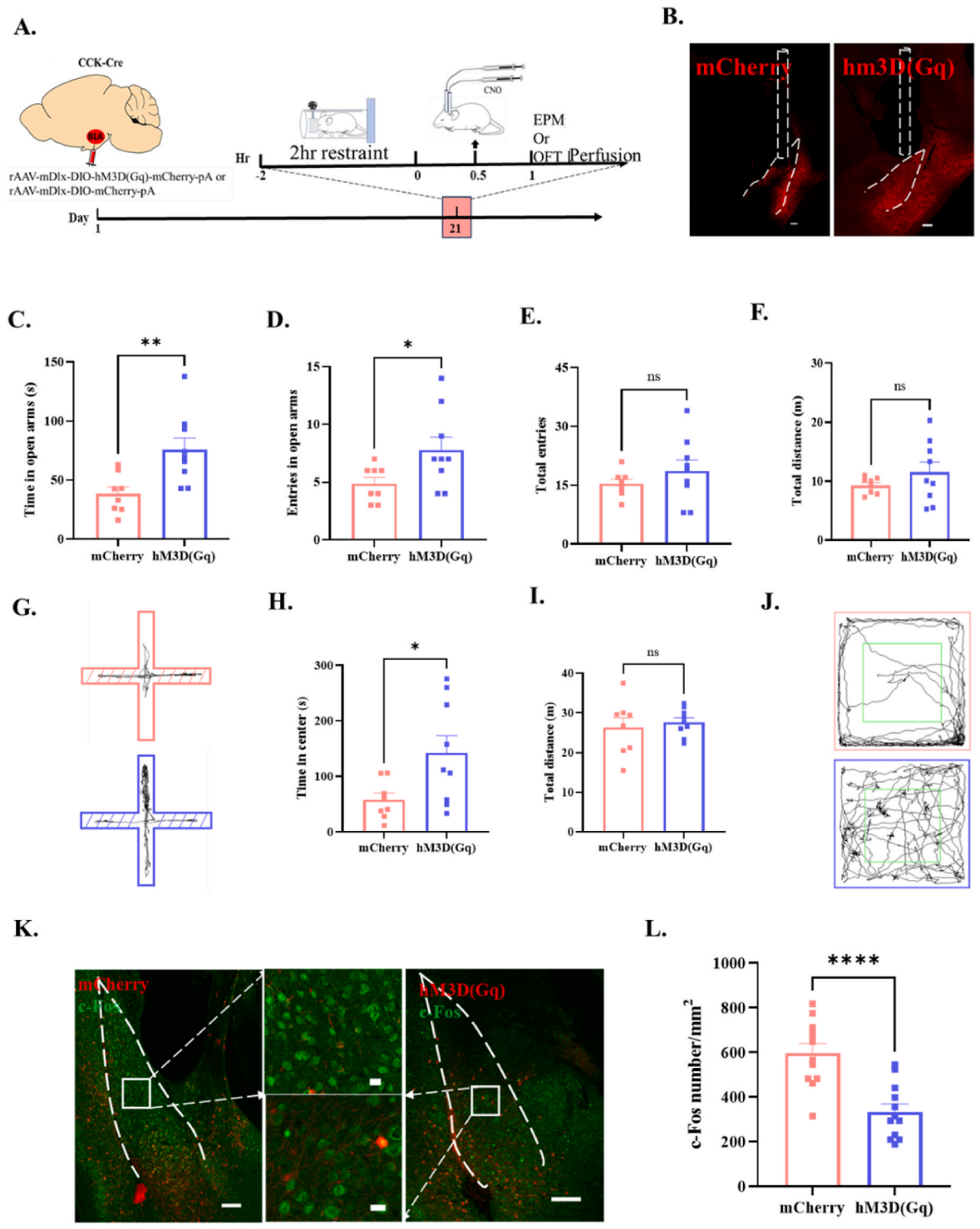

Fig. 3. Enhancing inhibitory transmission in BLA by Chemo-genetic activation of local CCK-INs can reduce anxiety-like behaviors in mice.
A, A schematic diagram shows the experimental design, including the timeline of virus injection and behavioral tests. **B,** Representative images show the virus expression in mCherry and hM3D(Gq) groups respectively. **C,** The bar chart shows the time mice (mCherry, N = 8; hM3D(Gq), N = 9) spent in the open arms in the elevated plus maze test (mCherry vs. hM3D(Gq): 38.46 ± 5.83 vs. 75.7 ± 10.03, t (15) = 3.11, p = 0.0072). **D,** The bar chart shows the number of entries in the open arms in the elevated plus maze test (mCherry vs. hM3D(Gq): 4.88 ± 0.55 vs. 7.78 ± 1.13, t (15) = 2.22, p = 0.0421). **E,** The bar chart shows the total number of entries in both open and closed arms in the elevated plus maze test (mCherry vs. hM3D(Gq): 15.38 ± 1.15 vs. 18.67 ± 2.76, t (15) = 1.05, p = 0.3102). **F,** The bar chart shows the total travelled time mice spent in the elevated plus maze test (mCherry vs. hM3D(Gq): 9.27 ± 0.49 vs. 11.51 ± 1.74, t (15) = 1.17, p = 0.2591). **G,** Representative movement traces in the elevated plus maze test. Pink: mCherry; Blue: hM3D(Gq). **H,** The bar chart shows the time mice spent in the center zone in the open field test (mCherry vs. hM3D(Gq): 57.53 ± 12.29 vs. 142.4 ± 31.05, t (15) = 2.42, p = 0.0284). **I,** The bar chart shows the total distance mice travelled in the open field test (mCherry vs. hM3D(Gq): 26.34 ± 2.45 vs. 27.66 ± 1.15, t (15) = 0.51, p = 0.6198). **J,** Representative movement traces in the open field test. **K,** Representative BLA c-Fos expression images from the mCherry (3 mice, 12 slices) and hM3D(Gq) groups (3 mice, 12 slices) **L,** The bar chart shows the quantification of c-Fos density (mCherry vs. hM3D(Gq): 597.5 ± 42.6 vs. 337 ± 35.14, t (22) = 4.78, p < 0.0001). ****p < 0.0001; **p < 0.01; *p < 0.05; ns: no significance. Scale bar: 200 μm and 20 μm. Data are shown as Mean ± SEM.

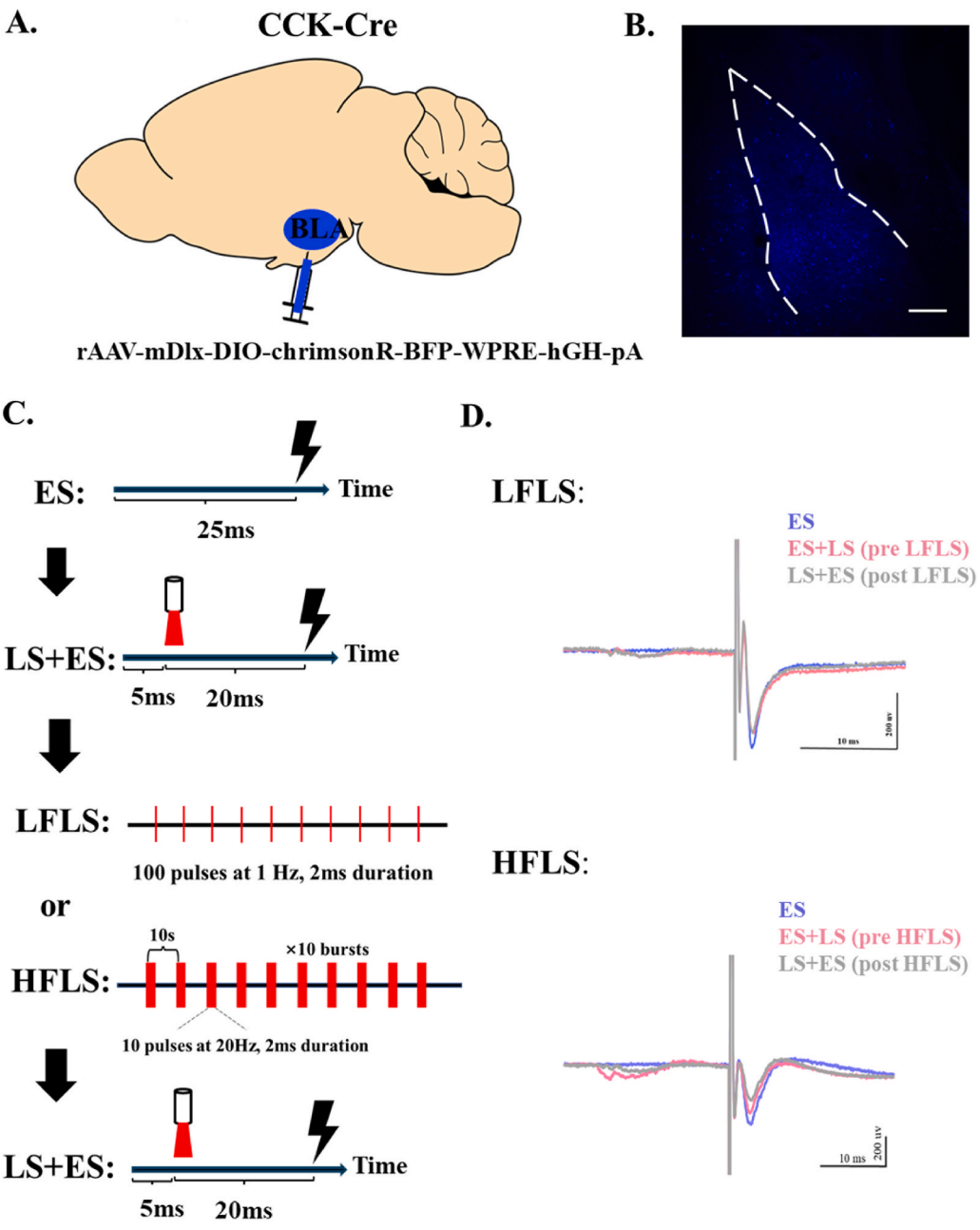

(caption on next page)

Fig. 4. HFLS but not LFLS of CCK-INs can induce iLTP in BLA.
A, A schematic diagram shows the injection of "rAAV-mDLX-DIO-ChrimsonR-BFP" into the BLA of CCK-Cre mice. **B,** A representative image shows the virus expression. **C,** A schematic diagram shows the protocol of in-vitro electrophysiology, including four sequential steps. In the first step ("ES"), we only presented an electrical stimulus (ES) with a 25 ms delay in each trial. In the second step ("LS + ES"), a laser stimulus (LS) was presented with a 5 ms delay and after 20 ms, the same ES was presented again. In the next step, we presented LFLS or HFLS, before which the slice was perfused with the vehicle for 10 min. In the last step, we presented the same pair of LS and ES as those in the second step. **D,** The representative fEPSP traces in "ES", "LS + ES (pre-HFLS)" and "LS + ES (post-HFLS)" steps in the LFLS and HFLS conditions. **E,** Left panel: The graph shows the change of the average normalized amplitude of fEPSP over time. Right panel: The bar chart shows the average values of normalized amplitudes of fEPSPs in the last 10 min of the three steps in the LFLS and HFLS conditions (RM two-way ANOVA with the Bonferroni post hoc tests, significant interaction effect: $F(2, 28) = 46.12$, $p < 0.0001$; the post hoc test reveals that in the LFLS condition, ES vs. LS + ES (pre-LFLS): 100.5% ± 0.26% vs. 85.51% ± 1.38%, $p < 0.0001$, while LS + ES (pre-LFLS) vs. LS + ES (post-LFLS): 85.51% ± 1.38% vs. 85.71% ± 2.75%, $p = 0.9365$; in the HFLS condition, ES vs. LS + ES (pre-HFLS): 100% ± 0.47% vs. 84.5% ± 3.17%, $p < 0.0001$, while LS + ES (pre-HFLS) vs. LS + ES (post-HFLS): 84.5% ± 3.17% vs. 55.97% ± 3.38%, $p < 0.0001$). LFLS: N = 4 mice, n = 8 slices; HFLS: N = 3 mice, n = 8 slices. ****$p < 0.0001$; ns: no significance. Scale bar: 200 μm. Data are shown as Mean ± SEM.

there was no significant difference in their travelled distance in both arms (Fig. 5F; mCherry vs. ChrimsonR: 9.07 ± 1.11 vs. 10.46 ± 0.53, $t(15) = 1.78$, $p = 0.2574$). Moreover, in the open field test, ChrimsonR mice spent more time in the center of open field (Fig. 5H–J; mCherry vs. ChrimsonR: 59.49 ± 5.2 vs. 119.4 ± 20.64, $t(15) = 2.66$, $p = 0.0178$) with similar travelled distances (Fig. 5I; mCherry vs. ChrimsonR: 30.04 ± 1.75 vs. 32.79 ± 2.57, $t(15) = 0.86$, $p = 0.4011$) than their control littermates. ChrimsonR mice also had weaker c-Fos expression in BLA than their control littermates (Fig. 5K and L; mCherry vs. ChrimsonR: 267.3 ± 27.81 vs. 152 ± 17.53, $t(22) = 3.51$, $p = 0.002$). Similarly, we also did not discover that HFLS of CCK-INs can affect the basal anxiety behaviors in mice (Fig. A6). For example, we found both mCherry and ChrimsonR mice did not have significant different travelled time spent in the open arms and center of the open field (Fig. A6B & F, EPM: mCherry vs. ChrimsonR: 26.58 ± 5.65 vs. 41.15 ± 4.69, $t(12) = 1.98$, $p = 0.0707$; Fig. A6G &I, OFT: mCherry vs. ChrimsonR: 79.77 ± 11.25 vs. 118.9 ± 32.24, $t(12) = 1.15$, $p = 0.2746$). They also did not differ in the entries of open arms and both arms (Fig. A6C, mCherry vs. ChrimsonR: 6.29 ± 1.19 vs. 7.43 ± 1.09, $t(12) = 0.71$, $p = 0.4919$; Fig. A6D, mCherry vs. ChrimsonR: 17.57 ± 2.17 vs. 19.14 ± 1.74, $t(12) = 0.57$, $p = 0.5823$) and travelled distance in the EPM (Fig. A6E, mCherry vs. ChrimsonR: 10.41 ± 0.92 vs. 10.7 ± 0.81, $t(12) = 0.23$, $p = 0.8204$) and OFT (Fig. A6H, mCherry vs. ChrimsonR: 30.09 ± 1.34 vs. 28.22 ± 3.21, $t(12) = 0.54$, $p = 0.6018$). There was also no significant difference in c-Fos expression between the groups (Fig. A6J & K, mCherry vs. ChrimsonR: 190.6 ± 15.27 vs. 161.2 ± 18.36, $t(22) = 1.23$, $p = 0.2326$). However, we also found a trend that ChrimsonR mice had lower basal anxiety level than mCherry mice. Likewise, we compared the behavioral performance between mCherry non-stressed and mCherry stressed groups. We found that mCherry non-stressed mice had more entries to the open arms (mCherry non-stressed vs. mCherry stressed: 6.29 ± 1.19 vs. 3.5 ± 0.57, $t(13) = 2.21$, $p = 0.046$) and less c-Fos signals in BLA (mCherry non-stressed vs. mCherry stressed: 190.6 ± 15.27 vs. 190.6 ± 15.27, $t(22) = 2.42$, $p = 0.0243$). We did not find significant difference in other behavioral indices (e.g., center time, time in open arms etc., ps > 0.05). These results suggest that ARS can also induce anxiety-like behaviors and BLA hyperactivity in the optogenetic experiment. Together, it can be concluded that the long-term inhibition induced by HFLS of CCK-INs in BLA can effectively alleviate stress-induced anxiety in mice but have limited effect on their basal anxiety levels.

4. Discussion

In this article, we show evidence to confirm the essential role of BLA CCK-INs in mediating anxiety. We found that CCK-INs in BLA send projections to most local excitatory neurons, which indicates the possible involvement of CCK-INs in modulating the excitatory neuronal activities in BLA. Further, we found enhancing the local inhibition by chemo-genetic or optogenetic activation CCK-INs can significantly suppress electrical stimulation-induced neuronal activities, which is supported by a previous finding that the neuronal activities of BLA excitatory neurons are mainly controlled by local GABAergic network (Prager et al., 2016).

Behaviorally, we found enhancing the local inhibition in BLA by direct and long-lasting activation of CCK-INs through chemo-genetics can reduce stress-induced anxiety-like behaviors in mice. The inhibitory control in BLA has been implicated in the regulation of anxiety-related behaviors (Prager et al., 2016; Truitt et al., 2009). For example, some researchers found the increased anxiety-like behaviors were associated with reduced inhibitory synaptic transmission (Chen et al., 2013; Truitt et al., 2009); the activation of interneurons in BLA can suppress the opposing valence-specific projection neurons to prevent the misinterpretation of a neutral or rewarding stimulus as threatening, which is a core symptom of anxiety disorders (Calhoon and Tye, 2015). Here, we further confirmed increasing CCK-GABAergic inhibitory transmission in BLA can reduce stress-induced anxiety-like behaviors in mice, which suggests decreased inhibitory transmission in BLA can lead to anxiety-like behaviors. Previous research found systematic activation of CCK-INs barely affected the basal anxiety-like behaviors in mice (Whissell et al., 2019), which is consistent to our results.

Previous studies found the iLTP induction in BLA required the activation of AMPAR and NMDAR (Bauer and LeDoux, 2004; Lange et al., 2012; Polepalli et al., 2010). We found iLTP induction in BLA also required the activation of GPR173. Our results revealed HFLS of CCK-INs in BLA can trigger iLTP, which can be blocked by GPR173 antagonists; LFLS of CCK-INs in BLA failed to trigger iLTP, but extra CCK8s application can rescue it. These results suggest that activation of GPR173 by CCK at CCK-GABAergic synapses is necessary for the iLTP induction in BLA. The same mechanisms of iLTP induction are also found in the neocortex (He et al., 2023). Moreover, we revealed that GPR173 mainly localizes at excitatory neurons rather than inhibitory neurons in BLA. We thereby propose that HFLS of CCK-INs may release CCK, which would bind to the postsynaptic GPR173 at excitatory neurons, triggering the induction of iLTP.

We further discovered that 10-min HFLS-induced iLTP can also alleviate stress-induced anxiety. A previous study has emphasized inhibitory plasticity is necessary to maintain the cortical neuronal excitation/inhibition (E/I) balance (Vogels et al., 2011). In our study, we adopted acute restraint stress to induce anxiety-like behaviors in mice and found it can also break the E/I balance in BLA to cause its hyperactivity. It can be inferred that inducing inhibitory plasticity in BLA can normalize the stress-induced E/I imbalance, producing reliable anxiolytic effects.

Except for chemo-genetics and optogenetics, CCK-INs can be indirectly modulated by presynaptic cannabinoid 1 (CB1) receptors which are mainly located at the CCK-IN terminals in BLA (Katona et al., 1999; McDonald and Mascagni, 2001; Nyiri et al., 2005). In-vitro studies showed that CB1 receptor agonists can inhibit GABA release from CCK-INs in BLA, suppressing local inhibitory transmission (Azad et al., 2003; Zhu and Lovinger, 2005). Knocking out CB1 receptors on cortical INs showed anxiolytic effects (Häring et al., 2011). However, intra-BLA infusion of CB1 receptor agonists also displayed anxiolytic effects (Tokutake et al., 2022; Zarrindast et al., 2012). Apart from inhibitory terminals, CB1 receptors also localized at excitatory terminals, modulating glutamatergic transmission (Yoshida et al., 2011), which may

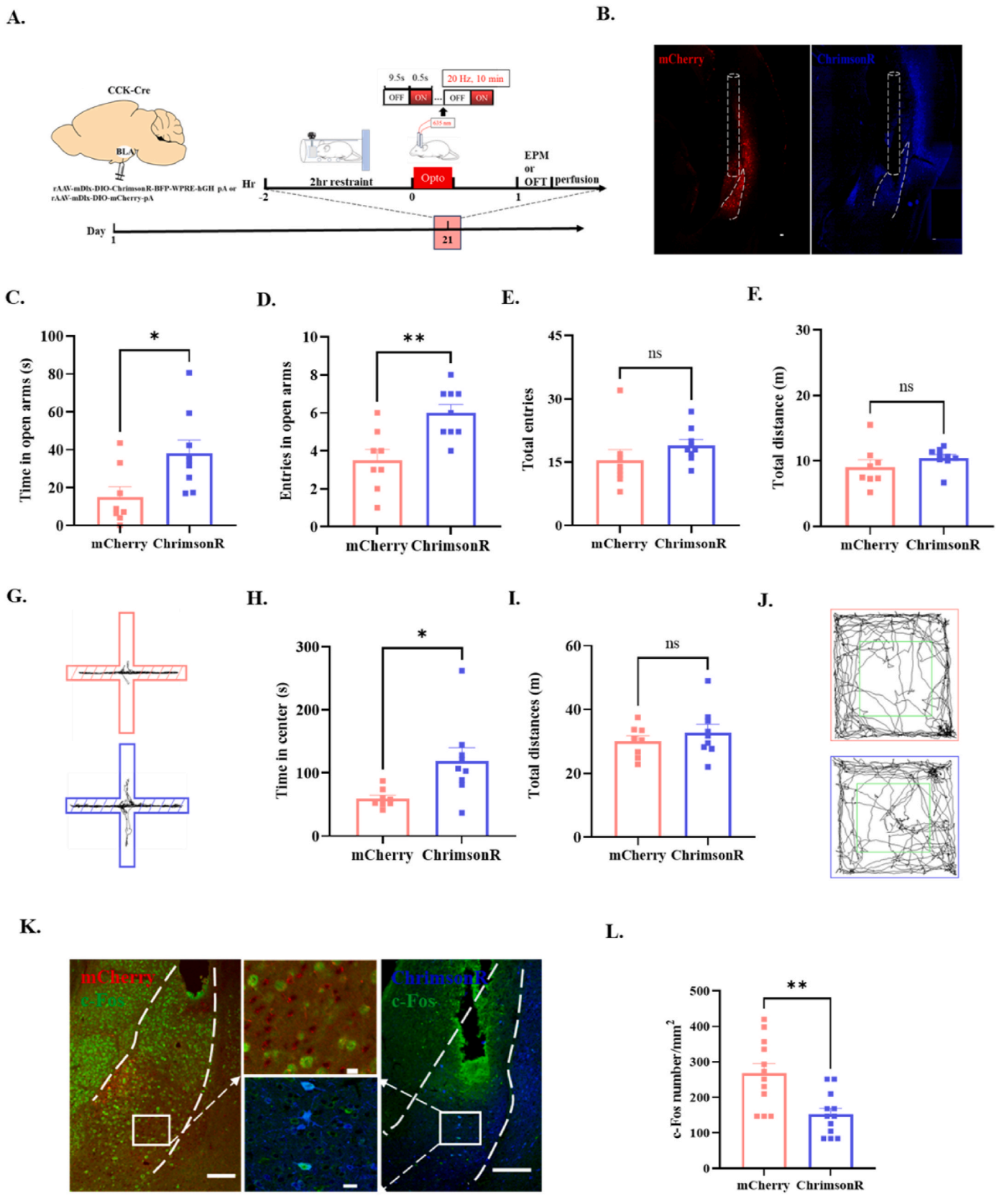

(caption on next page)

Fig. 5. Inducing inhibitory plasticity by HFLS of CCK-INs in BLA can reduce anxiety-like behaviors in mice.
A, A schematic diagram shows the experimental design, including a timeline of virus injection and behavioral tests. **B,** Representative images show the virus expression in mCherry and ChrimsonR groups respectively. **C,** The bar chart shows the time mice from the mCherry (N = 8) and ChrimsonR (N = 9) groups spent in the open arms in the elevated plus maze test (mCherry vs. ChrimsonR: 15.03 ± 5.45 vs. 38.28 ± 6.84, t (15) = 2.61, p = 0.0196). **D,** The bar chart shows the number of entries in the open arms in the elevated plus maze test (mCherry vs. ChrimsonR: 3.5 ± 0.57 vs. 6 ± 0.44, t (15) = 3.52, p = 0.0031). **E,** The bar chart shows the total number of entries in both arms in the elevated plus maze test (mCherry vs. ChrimsonR: 15.38 ± 2.58 vs. 19 ± 1.35, t (15) = 1.29, p = 0.2175). **F,** The bar chart shows the total travelled distance mice spent in the elevated plus maze test (mCherry vs. ChrimsonR: 9.07 ± 1.11 vs. 10.46 ± 0.53, t (15) = 1.78, p = 0.2574). **G,** The representative movement traces in the elevated plus maze test. Pink: mCherry; Blue: ChrimsonR. **H,** The bar chart shows the time mice spent in the center zone in the open field test (mCherry vs. ChrimsonR: 59.49 ± 5.2 vs. 119.4 ± 20.64, t (15) = 2.66, p = 0.0178). **I,** The bar chart shows the total distance mice travelled in the open field test (mCherry vs. ChrimsonR: 30.04 ± 1.75 vs. 32.79 ± 2.57, t (15) = 0.86, p = 0.4011). **J,** Representative movement traces in the open field test. **K,** Representative BLA c-Fos expression images from the mCherry (3 mice, 12 slices) and ChrimsonR groups (3 mice, 12 slices). **L,** The bar chart shows the quantification of c-Fos density (mCherry vs. ChrimsonR: 267.3 ± 27.81 vs. 152 ± 17.53, t (22) = 3.51, p = 0.002). **p < 0.01; *p < 0.05; ns: no significance. Scale bar: 200 μm and 20 μm. Data are shown as Mean ± SEM.

explain the anxiolytic effects of CB1 agonists. There were two main endocannabinoid (eCB) ligands acting on CB1 receptors, Anandamide (AEA) and 2-arachidonoylglycerol (2-AG) (Maccarrone and Finazzi-Agro, 2003). While AEA mainly targets CB1 receptors on glutamatergic terminals, controlling the presynaptic glutamate release and excitability of postsynaptic projection neurons (Hill and Tasker, 2012); 2-AG mainly acts on CB1 receptors on GABAergic terminals, regulating inhibitory transmission (Yasmin et al., 2020). Under stress, in BLA, AEA levels would decrease, and 2-AG concentration would increase, leading to stronger disinhibition of projection neurons (Yasmin et al., 2020). Previous research discovered that enhancing AEA signaling in BLA can rescue seizure-induced anxiety through normalizing seizure-induced dysfunctions of glutamatergic transmission (Colangeli et al., 2020). Moreover, Di et al. (2016) found that acute stress can activate CB1 receptors on CCK-INs in BLA through increasing the concentration of 2-AG, leading to decreased GABA release and distinct anxiety-like phenotypes. Interestingly, acute stress can facilitate the 2-AG release from ventral hippocampus - BLA synapses, which in turn activates the presynaptic CB1 receptors and improve stress-induced behaviors (Kondev et al., 2023). It suggests that under stress, both local and long-range eCB systems in BLA are involved in maintaining the local E/I balance. Moreover, CCK can decrease GABA release from CCK-INs in BLA through a CB1 receptor-mediated mechanism (Lee and Soltesz, 2011), which may be one of the causes of CCK anxiogenic effects in BLA (Pérez de la Mora et al., 2007).

Except for anxiety, CCK-INs in BLA are also implicated in fear extinction (Krabbe et al., 2018). Optogenetic activation of CCK-INs in BLA can promote fear extinction (Rovira-Esteban et al., 2019). There is a strong association between fear extinction and anxiety-like behaviors. For example, animals with slower fear extinction rates showed more intense anxiety-like behaviors after stress (Reznikov et al., 2015). The exposure therapy for anxiety disorders is based on fear extinction procedures (Graham and Milad, 2011). It indicates fear extinction dysfunctions may be one of the anxiety pathophysiology, which may need further research.

In this work, we respectively adopted chemo-genetics to activate CCK-INs in BLA to enhance local inhibitory transmission and optogenetics to HFLS of CCK-INs in BLA to enhance local inhibitory plasticity, which both can alleviate stress-induced anxiety-like behaviors in mice. Together, we discover that CCK-INs mediated inhibitory transmission and plasticity in BLA regulate stress-induced anxiety-like behaviors in mice, which further our understandings of pathophysiological mechanisms and therapeutic approaches for stress-induced anxiety disorders.

CRediT authorship contribution statement

Wei Fang: Conceptualization, Data curation, Formal analysis, Investigation, Methodology, Project administration, Software, Visualization, Writing – original draft, Writing – review & editing. **Xi Chen:** Writing – review & editing. **Jufang He:** Writing – review & editing, Supervision, Funding acquisition, Conceptualization.

Funding

This work was supported by funding from the following:

Hong Kong Research Grants Council, General Research Fund: CityU 11101521, CityU 11103922, CityU 11104923. Hong Kong Research Grants Council, Collaborative Research Fund: C1043-21G. Hong Kong Research Grants Council, Theme-Based Research Scheme: T13-605/18-W. Hong Kong Research Grants Council, Senior Research Fellow Scheme: SRFS2324-1S02. Innovation and Technology Fund of the Hong Kong SAR, China: GHP_075_19GD. Hong Kong Health Bureau, Health and Medical Research Fund: 09203656, 08194106. Innovation Technology Commission of the Hong Kong SAR, China: Health@InnoHK program.

Declaration of competing interest

The authors have no conflicts of interest to declare.

Acknowledgements

We would like to thank Ms. Chau Fong TSANG and Mr. Siu Hin LAU for their technical assistance in performing in-vitro electrophysiology. We value the comments from Dr. Wenjian Sun, Dr. Xuejiao ZHENG, and Dr. Fengwen HUANG. We also thank the following charitable foundations for their generous support to Prof. Jufang HE: Wong Chun Hong Endowed Chair Professorship, Charlie Lee Charitable Foundation, and Fong Shu Fook Tong Foundation.

Appendix A. Supplementary data

Supplementary data to this article can be found online at https://doi.org/10.1016/j.ynstr.2024.100680.

Data availability

Data will be made available on request.

References

Asim, M., Wang, H., Chen, X., He, J., 2023. Potentiated GABAergic neuronal activities in the basolateral amygdala alleviate stress-induced depressive behaviors. CNS Neurosci. Ther. 00, 1–15.

Azad, S.C., Eder, M., Marsicano, G., Lutz, B., Zieglgänsberger, W., Rammes, G., 2003. Activation of the cannabinoid receptor type 1 decreases glutamatergic and GABAergic synaptic transmission in the lateral amygdala of the mouse. Learn. Mem. 10 (2), 116–128.

Babaev, O., Piletti Chatain, C., Krueger-Burg, D., 2018. Inhibition in the amygdala anxiety circuitry. Exp. Mol. Med. 50 (4), 1–16.

Babij, R., Ferrer, C., Donatelle, A., Wacks, S., Buch, A.M., Niemeyer, J.E., Ma, H., Duan, Z.R.S., Fetcho, R.N., Che, A., 2023. Gabrb3 is required for the functional integration of pyramidal neuron subtypes in the somatosensory cortex. Neuron 111 (2), 256–274. e210.

Ballaz, S.J., Bourin, M., 2021. Cholecystokinin-mediated neuromodulation of anxiety and schizophrenia: a "dimmer-switch" hypothesis. Curr. Neuropharmacol. 19 (7), 925–938.

Bandelow, B., Michaelis, S., 2015. Epidemiology of anxiety disorders in the 21st century. Dialogues Clin. Neurosci. 17 (3), 327–335.
Bauer, E.P., LeDoux, J.E., 2004. Heterosynaptic long-term potentiation of inhibitory interneurons in the lateral amygdala. J. Neurosci. 24 (43), 9507–9512.
Calhoon, G.G., Tye, K.M., 2015. Resolving the neural circuits of anxiety. Nat. Neurosci. 18 (10), 1394–1404.
Chen, J., Song, Y., Yang, J., Zhang, Y., Zhao, P., Zhu, X.-J., Su, H.-c., 2013. The contribution of TNF-α in the amygdala to anxiety in mice with persistent inflammatory pain. Neurosci. Lett. 541, 275–280.
Colangeli, R., Morena, M., Pittman, Q.J., Hill, M.N., Teskey, G.C., 2020. Anandamide signaling augmentation rescues amygdala synaptic function and comorbid emotional alterations in a model of epilepsy. J. Neurosci. 40 (31), 6068–6081.
Creed, M., Pascoli, V.J., Lüscher, C., 2015. Refining deep brain stimulation to emulate optogenetic treatment of synaptic pathology. Science 347 (6222), 659–664.
Di, S., Itoga, C.A., Fisher, M.O., Solomonow, J., Roltsch, E.A., Gilpin, N.W., Tasker, J.G., 2016. Acute stress suppresses synaptic inhibition and increases anxiety via endocannabinoid release in the basolateral amygdala. J. Neurosci. 36 (32), 8461–8470.
Dooley, L.N., Slavich, G.M., Moreno, P.I., Bower, J.E., 2017. Strength through adversity: moderate lifetime stress exposure is associated with psychological resilience in breast cancer survivors. Stress Health 33 (5), 549–557.
Freund, T.F., 2003. Interneuron diversity series: rhythm and mood in perisomatic inhibition. Trends Neurosci. 26 (9), 489–495.
Graham, B.M., Milad, M.R., 2011. The study of fear extinction: implications for anxiety disorders. Am. J. Psychiatr. 168 (12), 1255–1265.
Häring, M., Kaiser, N., Monory, K., Lutz, B., 2011. Circuit specific functions of cannabinoid CB1 receptor in the balance of investigatory drive and exploration. PLoS One 6 (11), e26617.
Hawken, E., Normandeau, C., Gardner Gregory, J., Cécyre, B., Bouchard, J.-F., Mackie, K., Dumont, É., 2019. A novel GPR55-mediated satiety signal in the oval bed nucleus of the stria terminalis. Neuropsychopharmacology 44 (7), 1274–1283.
He, L., Shi, H., Zhang, G., Peng, Y., Ghosh, A., Zhang, M., Hu, X., Liu, C., Shao, Y., Wang, S., 2023. A novel CCK receptor GPR173 mediates potentiation of GABAergic inhibition. J. Neurosci. 43 (13), 2305–2325.
Hill, M.N., Tasker, J.G., 2012. Endocannabinoid signaling, glucocorticoid-mediated negative feedback, and regulation of the hypothalamic-pituitary-adrenal axis. Neuroscience 204, 5–16.
Ippolito, D.M., Eroglu, C., 2010. Quantifying synapses: an immunocytochemistry-based assay to quantify synapse number. JoVE (Journal of Visualized Experiments) (45), e2270.
Katona, I., Sperlagh, B., Sık, A., Käfalvi, A., Vizi, E.S., Mackie, K., Freund, T.F., 1999. Presynaptically located CB1 cannabinoid receptors regulate GABA release from axon terminals of specific hippocampal interneurons. J. Neurosci. 19 (11), 4544–4558.
Kemppainen, S., Pitkänen, A., 2000. Distribution of parvalbumin, calretinin, and calbindin-D28k immunoreactivity in the rat amygdaloid complex and colocalization with γ-aminobutyric acid. J. Comp. Neurol. 426 (3), 441–467.
Kondev, V., Najeed, M., Yasmin, F., Morgan, A., Loomba, N., Johnson, K., et al., 2023. Endocannabinoid release at ventral hippocampal-amygdala synapses regulates stress-induced behavioral adaptation. Cell Rep. 42 (9).
Krabbe, S., Gründemann, J., Lüthi, A., 2018. Amygdala inhibitory circuits regulate associative fear conditioning. Biol. Psychiatr. 83 (10), 800–809.
Lange, M., Doengi, M., Lesting, J., Pape, H., Jüngling, K., 2012. Heterosynaptic long-term potentiation at interneuron–principal neuron synapses in the amygdala requires nitric oxide signalling. J. Physiol. 590 (1), 131–143.
Lee, S.H., Soltesz, I., 2011. Requirement for CB1 but not GABAB receptors in the cholecystokinin mediated inhibition of GABA release from cholecystokinin expressing basket cells. J. Physiol. 589 (4), 891–902.
Lee, I.C., Yu, T.H., Liu, W.H., Hsu, K.S., 2021. Social transmission and buffering of hippocampal metaplasticity after stress in mice. J. Neurosci. 41 (6), 1317–1330.
Liu, W.-Z., Huang, S.-H., Wang, Y., Wang, C.-Y., Pan, H.-Q., Zhao, K., Hu, P., Pan, B.-X., Zhang, W.-H., 2023. Medial prefrontal cortex input to basolateral amygdala controls acute stress-induced short-term anxiety-like behavior in mice. Neuropsychopharmacology 48 (5), 734–744.
Lochner, C., Mogotsi, M., du Toit, P.L., Kaminer, D., Niehaus, D.J., Stein, D.J., 2003. Quality of life in anxiety disorders: a comparison of obsessive-compulsive disorder, social anxiety disorder, and panic disorder. Psychopathology 36 (5), 255–262.
Luo, Z.-Y., Huang, L., Lin, S., Yin, Y.-N., Jie, W., Hu, N.-Y., Hu, Y.-Y., Guan, Y.-F., Liu, J.-H., You, Q.-L., 2020. Erbin in amygdala parvalbumin-positive neurons modulates anxiety-like behaviors. Biol. Psychiatr. 87 (10), 926–936.
Maccarrone, M., Finazzi-Agro, A., 2003. The endocannabinoid system, anandamide and the regulation of mammalian cell apoptosis. Cell Death Differ. 10 (9), 946–955.
McDonald, A., Mascagni, F., 2001. Localization of the CB1 type cannabinoid receptor in the rat basolateral amygdala: high concentrations in a subpopulation of cholecystokinin-containing interneurons. Neuroscience 107 (4), 641–652.
Miska, N.J., Richter, L.M., Cary, B.A., Gjorgjieva, J., Turrigiano, G.G., 2018. Sensory experience inversely regulates feedforward and feedback excitation-inhibition ratio in rodent visual cortex. Elife 7, e38846.
Möhler, H., 2012. The GABA system in anxiety and depression and its therapeutic potential. Neuropharmacology 62 (1), 42–53.
Muller, J.F., Mascagni, F., McDonald, A.J., 2007. Postsynaptic targets of somatostatin-containing interneurons in the rat basolateral amygdala. J. Comp. Neurol. 500 (3), 513–529.
Mustafa, T., Jiang, S.Z., Eiden, A.M., Weihe, E., Thistlethwaite, I., Eiden, L.E., 2015. Impact of PACAP and PAC1 receptor deficiency on the neurochemical and behavioral effects of acute and chronic restraint stress in male C57BL/6 mice. Stress 18 (4), 408–418.
Nahmani, M., Turrigiano, G.G., 2014. Adult cortical plasticity following injury: recapitulation of critical period mechanisms? Neuroscience 283, 4–16.
Nonaka, H., Sakamoto, S., Shiraiwa, K., Ishikawa, M., Tamura, T., Okuno, K., Kondo, T., Kiyonaka, S., Susaki, E.A., Shimizu, C., 2024. Bioorthogonal chemical labeling of endogenous neurotransmitter receptors in living mouse brains. Proc. Natl. Acad. Sci. USA 121 (6), e2313887121.
Novaes, L.S., Dos Santos, N.B., Perfetto, J.G., Goosens, K.A., Munhoz, C.D., 2018. Environmental enrichment prevents acute restraint stress-induced anxiety-related behavior but not changes in basolateral amygdala spine density. Psychoneuroendocrinology 98, 6–10.
Nyiri, G., Cserép, C., Szabadits, E., Mackie, K., Freund, T., 2005. CB1 cannabinoid receptors are enriched in the perisynaptic annulus and on preterminal segments of hippocampal GABAergic axons. Neuroscience 136 (3), 811–822.
Oshri, A., Cui, Z., Owens, M.M., Carvalho, C.A., Sweet, L., 2022. Low-to-moderate level of perceived stress strengthens working memory: testing the hormesis hypothesis through neural activation. Neuropsychologia 176, 108354.
Pérez de la Mora, M., Hernández-Gómez, A.M., Arizmendi-García, Y., Jacobsen, K.X., Lara-García, D., Flores-Gracia, C., Crespo-Ramírez, M., Gallegos-Cari, A., Nuche-Bricaire, A., Fuxe, K., 2007. Role of the amygdaloid cholecystokinin (CCK)/gastrin-2 receptors and terminal networks in the modulation of anxiety in the rat. Effects of CCK-4 and CCK-8S on anxiety-like behaviour and [3H] GABA release. Eur. J. Neurosci. 26 (12), 3614–3630.
Polepalli, J.S., Sullivan, R.K., Yanagawa, Y., Sah, P., 2010. A specific class of interneuron mediates inhibitory plasticity in the lateral amygdala. J. Neurosci. 30 (44), 14619–14629.
Prager, E.M., Bergstrom, H.C., Wynn, G.H., Braga, M.F., 2016. The basolateral amygdala γ-aminobutyric acidergic system in health and disease. J. Neurosci. Res. 94 (6), 548–567.
Rainnie, D.G., Mania, I., Mascagni, F., McDonald, A.J., 2006. Physiological and morphological characterization of parvalbumin-containing interneurons of the rat basolateral amygdala. J. Comp. Neurol. 498 (1), 142–161.
Reznikov, R., Diwan, M., Nobrega, J.N., Hamani, C., 2015. Towards a better preclinical model of PTSD: characterizing animals with weak extinction, maladaptive stress responses and low plasma corticosterone. J. Psychiatr. Res. 61, 158–165.
Rovira-Esteban, L., Gunduz-Cinar, O., Bukalo, O., Limoges, A., Brockway, E., Müller, K., Fenno, L., Kim, Y.S., Ramakrishnan, C., Andrási, T., 2019. Excitation of diverse classes of cholecystokinin interneurons in the basal amygdala facilitates fear extinction. Eneuro 6 (6).
Seibenhener, M.L., Wooten, M.C., 2015. Use of the open field maze to measure locomotor and anxiety-like behavior in mice. JoVE (Journal of Visualized Experiments) (96), e52434.
Spampanato, J., Polepalli, J., Sah, P., 2011. Interneurons in the basolateral amygdala. Neuropharmacology 60 (5), 765–773.
Su, J., Huang, F., Tian, Y., Tian, R., Gao, Q., Bello, S.T., Zeng, D., Jendrichovsky, P., Lau, C.G., Xiong, W., Yu, D., Tortorella, M., Chen, X., He, J., 2023. Entorhinohippocampal cholecystokinin modulates spatial learning by facilitating neuroplasticity of hippocampal CA3-CA1 synapses. Cell Rep. 42 (12).
Tokutake, T., Asano, T., Miyanishi, H., Nakaya, S., Izuo, N., Nitta, A., 2022. Cannabinoid type 1 receptors in the basolateral amygdala regulate ACPA-induced place preference and anxiolytic-like behaviors. Neurochem. Res. 47 (9), 2899–2908.
Truitt, W.A., Johnson, P.L., Dietrich, A.D., Fitz, S.D., Shekhar, A., 2009. Anxiety-like behavior is modulated by a discrete subpopulation of interneurons in the basolateral amygdala. Neuroscience 160 (2), 284–294.
Vereczki, V.K., Müller, K., Krizsán, É., Máté, Z., Fekete, Z., Rovira-Esteban, L., Veres, J. M., Erdélyi, F., Hájos, N., 2021. Total number and ratio of GABAergic neuron types in the mouse lateral and basal amygdala. J. Neurosci. 41 (21), 4575–4595.
Vereczki, V.K., Veres, J.M., Müller, K., Nagy, G.A., Rácz, B., Barsy, B., Hájos, N., 2016. Synaptic organization of perisomatic GABAergic inputs onto the principal cells of the mouse basolateral amygdala. Front. Neuroanat. 10, 20.
Vogels, T.P., Sprekeler, H., Zenke, F., Clopath, C., Gerstner, W., 2011. Inhibitory plasticity balances excitation and inhibition in sensory pathways and memory networks. Science 334 (6062), 1569–1573.
Walf, A.A., Frye, C.A., 2007. The use of the elevated plus maze as an assay of anxiety-related behavior in rodents. Nat. Protoc. 2 (2), 322–328.
Whissell, P.D., Bang, J.Y., Khan, I., Xie, Y.-F., Parfitt, G.M., Grenon, M., Plummer, N.W., Jensen, P., Bonin, R.P., Kim, J.C., 2019. Selective activation of cholecystokinin-expressing GABA (CCK-GABA) neurons enhances memory and cognition. Eneuro 6 (1).
Wright, C.J., Milosavljevic, S., Pocivavsek, A., 2023. The stress of losing sleep: sex-specific neurobiological outcomes. Neurobiology of stress 24, 100543.
Wu, Y.K., Miehl, C., Gjorgjieva, J., 2022. Regulation of circuit organization and function through inhibitory synaptic plasticity. Trends Neurosci. 45 (12), 884–898..
Yasmin, F., Colangeli, R., Morena, M., Filipski, S., van der Stelt, M., Pittman, Q.J., Hillard, C.J., Teskey, G.C., McEwen, B.S., Hill, M.N., 2020. Stress-induced modulation of endocannabinoid signaling leads to delayed strengthening of synaptic connectivity in the amygdala. Proc. Natl. Acad. Sci. USA 117 (1), 650–655.
Yeung, M., Engin, E., Treit, D., 2011. Anxiolytic-like effects of somatostatin isoforms SST 14 and SST 28 in two animal models (Rattus norvegicus) after intra-amygdalar and intra-septal microinfusions. Psychopharmacology 216, 557–567.
Yoshida, T., Uchigashima, M., Yamasaki, M., Katona, I., Yamazaki, M., Sakimura, K., Kano, M., Yoshioka, M., Watanabe, M., 2011. Unique inhibitory synapse with particularly rich endocannabinoid signaling machinery on pyramidal neurons in basal amygdaloid nucleus. Proc. Natl. Acad. Sci. USA 108 (7), 3059–3064.
Zarrindast, M., Ghiasvand, M., Rezayof, A., Ahmadi, S., 2012. The amnesic effect of intra-central amygdala administration of a cannabinoid CB1 receptor agonist, WIN55,

212-2, is mediated by a beta-1 noradrenergic system in rat. Neuroscience 212, 77–85.
Zhang, X., Asim, M., Fang, W., Md Monir, H., Wang, H., Kim, K., Feng, H., Wang, S., Gao, Q., Lai, Y., 2023. Cholecystokinin B receptor antagonists for the treatment of depression via blocking long-term potentiation in the basolateral amygdala. Mol. Psychiatr. 1–16.
Zhu, P.J., Lovinger, D.M., 2005. Retrograde endocannabinoid signaling in a postsynaptic neuron/synaptic bouton preparation from basolateral amygdala. J. Neurosci. 25 (26), 6199–6207.